Title

The evolution of antimicrobial peptide resistance in *Pseudomonas aeruginosa* is severely constrained by random peptide mixtures

Authors

B. Antunes[1,2,*], C. Zanchi[1,*], B. Maron[2], C. Witzany[3], R. Regoes[3], Z. Hayouka[2,#] and J. Rolff[1, #]

[1] Freie Universität Berlin, Evolutionary Biology, Königin-Luise-Straße 1-3, 14195 Berlin, Germany.

[2] Institute of Biochemistry, Food Science and Nutrition, The Hebrew University of Jerusalem, Rehovot, Israel.

[3] Institute of Integrative Biology, ETH Zurich, Zurich, Switzerland.

* Co-first authors.

[#] Corresponding authors: Zvi Hayouka (zvi.hayouka@mail.huji.ac.il) and Jens Rolff (jens.rolff@fu-berlin.de).

Abstract

The prevalence of antibiotic-resistant pathogens has become a major threat to public health, requiring swift initiatives for discovering new strategies to control bacterial infections. Hence, antibiotic stewardship and rapid diagnostics, but also the development, and prudent use, of novel effective antimicrobial agents are paramount. Ideally, these agents should be less likely to select for resistance in pathogens than currently available conventional antimicrobials. The usage of antimicrobial Peptides (AMPs), key components of the innate immune response, and combination therapies, have been proposed as strategies to diminish the emergence of resistance.

Herein, we investigated whether newly developed random antimicrobial peptide mixtures (RPMs) can significantly reduce the risk of resistance evolution *in vitro* to that of single sequence AMPs, using the ESKAPE pathogen *Pseudomonas aeruginosa* (*P. aeruginosa*) as a model Gram-negative bacterium. Infections of this pathogen are difficult to treat due the inherent resistance to many drug classes, enhanced by the capacity to form biofilms. *P. aeruginosa* was experimentally evolved in the presence of AMPs or RPMs, subsequentially assessing the extent of resistance evolution and cross-resistance/collateral sensitivity between treatments. Furthermore, the fitness

costs of resistance on bacterial growth were studied, and whole-genome sequencing used to investigate which mutations could be candidates for causing resistant phenotypes. Lastly, changes in the pharmacodynamics of the evolved bacterial strains were examined.

Our findings suggest that using RPMs bears a much lower risk of resistance evolution compared to AMPs and mostly prevents cross-resistance development to other treatments, while maintaining (or even improving) drug sensitivity. This strengthens the case for using random cocktails of AMPs in favour of single AMPs, against which resistance evolved *in vitro*, further providing an alternative to classic antibiotics worth pursuing.

Introduction

The prevalence of antibiotic-resistant pathogens has become a major threat to public health, with an estimated 4.95 million deaths associated with drug-resistant bacteria in 2019 (1). Although resistance is a natural development, misuse and overuse of antibiotics has accelerated evolutionary selection and resistance, decreasing the efficiency of available antibiotics (2, 3). Hence, there is a strong incentive to discover new strategies to control bacterial infections, such as antibiotic stewardship and rapid diagnostics, but also the development, and prudent use, of novel effective antimicrobial agents (4, 5). An important and desirable feature of such agents would be a much lower risk to select for drug resistance in pathogens than currently available conventional antimicrobials. This would make the use of such drugs much more sustainable.

Antimicrobial Peptides (AMPs) form an important component of the innate immune response in multicellular organisms and have been frequently proposed as new antimicrobial drug candidates (6). These peptides usually have spatially explicit hydrophobic and cationic residues, which promote their ability to disrupt bacterial membranes (7, 8). Fundamentally, while hydrophobic residues interact with the hydrophobic interior of the lipid bilayer, their high net cationic charge selects prokaryotic membranes over eukaryotic cells (9, 10). AMPs range across the tree of life, showing a surprising diversity and variety in size and form (11). Moreover, while resistance has been shown to evolve against these antimicrobial agents, it evolves at a much slower rate than conventional antibiotics (12-14). Interestingly, for colistin, an AMP of bacterial origin that has been used for more than sixty years (15), it took around fifty years between the introduction and the spread of resistance (16).

61 In the current antibiotic crisis, bacterial pathogens are increasingly resistant to the available
62 monotherapeutical antibiotic drugs, often evolved through redundant mechanisms and to multiple
63 antibiotics in the same organism (17). This situation has been exacerbated by misuse and lack of
64 innovation in the discovery of new, and effective, antibiotic agents (18). Hence, combination
65 therapies have been explored and shown, by multitarget engagement, to diminish the emergence
66 of spontaneous resistance (19, 20). Among novel strategies under scrutiny is the usage of newly
67 developed random antimicrobial peptide mixtures (RPMs) (21, 22).
68 The broad molecular diversity of AMPs suggests that their prokaryotic-selective activity does not
69 depend on specific features of amino acid sequence or peptide conformation (8). Hence, research
70 groups have developed novel approaches to synthesize RPMs, using a solution containing
71 defined concentrations of hydrophobic and cationic amino acids (21, 23). This results in 2^n peptide
72 sequences (where n is the number of coupling steps and the chain length of the peptides). These
73 random peptide libraries, composed of hydrophobic and cationic amino acids, have shown strong
74 antimicrobial activity against multiple gram-negative and positive bacteria, including multi-drug
75 resistant (MDR), methicillin-resistant *Staphylococcus aureus* (MRSA), vancomycin-resistant
76 *Enterococci* (VRE), *Listeria monocytogenes* and several plant pathogenic bacteria (24-27).
77 Moreover, some attention has been given to a subfamily of AMPs with strong antimicrobial activity
78 – lipopeptides. Lipopeptides are produced non-ribosomally in bacteria and fungi, consisting of a
79 short linear or cyclic peptide sequence to which a fatty acid moiety is covalently attached at the
80 N-terminus (28). Synthetic ultrashort lipopeptides have shown broad antimicrobial activity towards
81 human pathogenic yeast, fungi and bacteria, as well as plant pathogenic fungi and bacteria (29,
82 30). RPMs of synthetic lipopeptides have also been studied by Topman-Rakover et al., displaying
83 broad antimicrobial activity against gram-negative and gram-positive bacteria, without causing
84 cytotoxicity to mammalian cells or plants (25, 26).
85 Here, we studied whether a treatment strategy based on the usage of RPMs and lipo-RPMs, can
86 significantly reduce the risk of resistance evolution *in vitro*, compared to AMPs. We used the
87 ESKAPE pathogen *Pseudomonas aeruginosa* (*P. aeruginosa*) as a model gram-negative
88 bacterium (31). This opportunistic pathogen is involved in chronic respiratory infections,
89 particularly those associated with cystic fibrosis, as well as hospital-acquired infections (32). *P.*
90 *aeruginosa* infections are difficult to treat due the inherent resistance to many drug classes,

enhanced by the capacity to form sessile microcolonies that stick to a surface and each other, eventually forming biofilms (33, 34). Resistance associated *P. aeruginosa* deaths were estimated around 300 thousand in 2019 (1).

We allowed *P. aeruginosa* to experimentally evolve in the presence of AMPs or RPMs. The selection covered 4 weeks, which is consistent with treatment regimens of *P. aeruginosa* infections (35). At the end of the experimental evolution course, we measured the extent of resistance evolution and whether the evolved strains showed cross-resistance/collateral sensitivity to the AMPs and RPMs. We also assessed the fitness costs of resistance on bacterial growth, and used whole-genome sequencing to investigate which mutations could be candidates for causing resistant phenotypes. Finally, we investigated changes in the pharmacodynamics of the evolved bacterial strains (12, 36, 37).

The usage of random peptide libraries (i.e. RPMs) instead of homogeneous peptides (i.e. one sequence, one chain length and one stereochemistry) offers some practical advantages, as the chemical synthesis of sequence-specific oligomers is more difficult and expensive than copolymerization (21). Hence, this study aims not only to provide in-depth insight on RPMs as novel alternatives to classical antibiotics, but also to how they fare in comparison to single sequence AMPs. Our findings suggest that using RPMs results in a much lower probability of resistance evolution and mostly prevents cross-resistance development to other treatments, while maintaining (or even increasing) drug sensitivity.

Results

1. <u>RPMs slow down resistance evolution.</u>

The evolution of resistance in *P. aeruginosa 14* (PA14) was investigated against nine antimicrobials: 6 single sequence AMPs and 3 RPMs, with diverse modes of action, all active against PA14 (by standard MIC assays; Table S1). The level of resistance was determined based on the change of the MIC of the evolved strains in comparison to the previously determined MIC of the ancestor strain ("MIC fold-change"; Table S1). The selection regime was found to influence MIC fold-changes across the different evolved strains ($X^2_{17.88}=565.4$; $p<0.0001$; Fig. 1 and S5). We found that all AMPs select for resistance when compared to their respective control (i.e. MIC fold-change is significantly different from the MIC fold-change of the control, when exposed to the

121 same AMP). Among the RPMs, only p-FdK5 20/80 showed a significant difference compared to
122 the control. The magnitude of the difference between evolved and control is much lower for the 3
123 RPMs compared to all the single sequence AMPs.

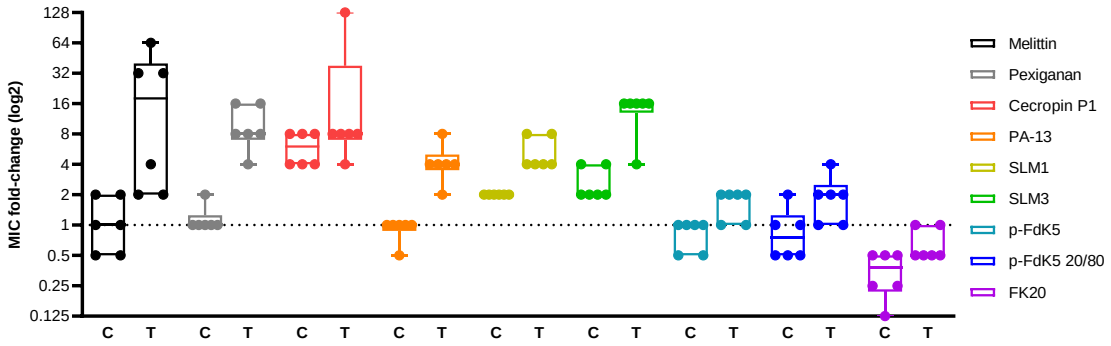

124 *Figure 1 – Resistance evolves slower in RPMs, when compared with single sequence AMPs. Resistance*
125 *determined by MIC assay of each evolved strain towards the corresponding peptide ("T" represents treated groups and "C" the control exposed to the respective treatment). Results shown as log2 fold-*
126 *change of the ancestor MICs. The boxes span the range between the 25th and 75th percentile, while the horizontal line inside represents the median value. The vertical bars extend to the minimum and*
127 *maximum score, excluding outliers (n=6; $X^2_{17,88}$ = 565,4; p<0.0001). The results represent two independent experiments.*

128 Additionally, under this experimental setting, the resistance to Cecropin P1 seems to evolve
129 readily, as the control strain showed a significantly higher MIC fold-change when exposed to
130 Cecropin P1 than in any other AMPs/RPMs-exposed control. The opposite effect can be seen in
131 the FK20 treatment, in which the control strain shows the lowest MIC fold-change.
132 Overall, FK20 out-performed all the other peptides in hindering resistance evolution, including
133 both 5-mer lipo-RPMs p-FdK5 and p-FdK5 20/80. Among single sequence AMPs, PA-13 and
134 SLM1 performed best, leading to a lower MIC fold-change compared to the other AMPs. *Post hoc*
135 analysis shows that RPMs reduce resistance evolution better than single sequence AMPs (Fig.
136 S5), particularly evident for FK20-evolved strains.

137 2. <u>Most evolved strains display collateral sensitivity to FK20.</u>

138 In the case of cross-resistance, evolution of resistance to one drug can increase bacterial fitness
139 to other drugs, while the opposite is known as collateral sensitivity (38, 39). To investigate this in
140 our experimentally evolved strains, they were exposed to the other antimicrobials of our panel
141 (Fig. 2). Across the board, strains evolved against Melittin, Pexiganan, Cecropin P1 and PA13
142 retained sensitivity to FK20, as did strains evolved in the presence of FK20. Furthermore,
143 Cecropin P1-evolved strains, despite being resistant to Cecropin P1, did not show cross-
144 resistance towards Melittin, Pexiganan and PA-13. On the other hand, strains evolved in the

145 presence of Melittin and Pexiganan, PA13 and FK 20 were cross-resistant to Cecropin P1, the
146 most resistant strains being the ones evolved in the presence of Melittin and Pexiganan.

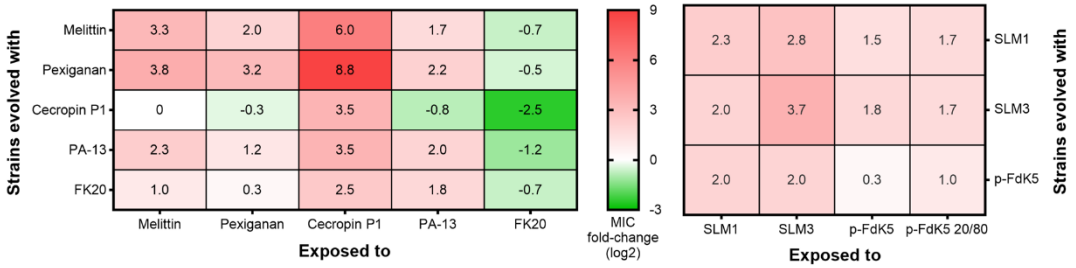

147

148 *Figure 2 – Cross-resistance evolved frequently against Cecropin P1, but collateral sensitivity steadily evolved towards FK20. A standard MIC assay was performed to evaluate the cross-resistance and collateral sensitivity. In each experiment, the evolved strains were exposed to different AMPs/RPMs,*
149 *using the selected AMP/RPM as control. The MIC values are represented as the mean fold-change (log2) of the ancestor's MIC. The results represent two independent experiments (n=6). Red colour represents*
150 *cross-resistance and green indicates collateral sensitivity.*

151 Cross-resistance/collateral sensitivity of bacterial strains evolved in the presence of lipopeptides
152 against other lipopeptides of our panel (SLM1, SLM3 and lipo-RPMs p-FdK5 and p-FdK5 20/20)
153 was also evaluated. We detected no observable collateral sensitivity towards the remaining
154 palmitic acid-modified peptides (Fig. 2). Nonetheless, despite great amino acid sequence
155 similarity between peptides (Table S1), only moderate levels of cross-resistance were observed
156 for lipo-AMPs/-RPMs. Nonetheless, the level of cross-resistance between palmitic acid modified
157 peptides is of far lesser magnitude than the level of cross-resistance towards Cecropin P1
158 exhibited by strains selected for other peptides.

159 3. <u>Lower resistance evolution leads to extended lag time.</u>

160 The fitness cost associated with the evolution of PA14 in presence, or absence, of AMP/RPMs
161 was investigated and the parameters, lag time and maximum growth rate (Vmax), were
162 normalised to those of the ancestor strain (i.e. fold-change; Fig. S1). There was a significant effect
163 of the selection regime on the lag time fold-change (Fig. S1-A; $X^2_{9,40} = 44,31$; $p<0.0001$), namely,
164 Pexiganan-, PA-13-, SLM3- and FK20-evolved strains display significantly increased lag times,
165 compared to control strains (Fig. S1-A and S6). There was, however, no effect of the experimental
166 evolution regime on the maximum growth rate (Vmax) of the strains (Fig. S1-B; $X^2_{9,40} = 11,9$;
167 $p=0.22$).

168

169

4. Mutations evolved in all treatments.

To better understand the mechanisms responsible for resistance evolution (or absence thereof), the genomic DNA of evolved strains was sequenced and compared to the assembled genome of the ancestor strain of PA14. A heat-map summary of the emerged mutations in evolved strains (including control) can be found in Fig. S2. Sequencing revealed that the majority of occurring SNPs were present in five genes (84%): *lasR*, *phoQ*, *tpbB*, *oprL* and *wbpA* (Fig. 3; strains without mutations were also plotted for comparison). In this section, cross-resistance/collateral sensitivity data was used to explore whether the SNPs in these 5 genes were associated with resistance to the panel of tested antimicrobials. Specifically, we tested whether presence/absence of a SNP, in each of the 5 genes, explained MIC fold-changes towards individual antimicrobial treatments, among the bacterial strains of all selection regimes. Interestingly, among these 5 genes, *tpbB* and *oprL* presented SNPs in only 1 of the 2 replicates of the experiment. Additionally, the software tool Provean was used to predict whether an amino acid substitution, or indel, affected the biological function of the target protein (40).

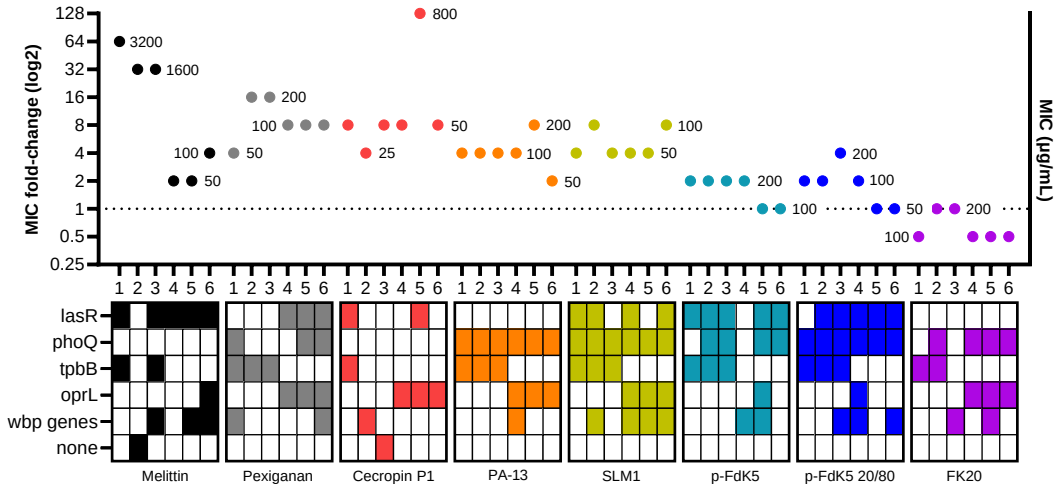

Figure 3 – Representation of the resistance evolution (MIC fold-changes) in relation to the presence/absence of mutations in the 5 most frequently mutated genes. Results shown as log2 fold-change of the ancestor MICs; Each dot represents the mean of triplicates (values beside the dots represent the MIC value). The x-axis displays individual strains per treatment and the respective mutations (or absence of) are portrayed underneath. The results represent two independent experiments. Evolved mutations against FK20 did not result in resistant strains.

TpbB is a diguanylate cyclase which is directly involved in the formation small colony variants (SCVs) in P. aeruginosa (41). A single type of SNPs was found in the *tpbB* gene, resulting in an amino acid substitution (valine to alanine in position 40), deemed not to affect protein function by

191 Provean. *TpbB* gene mutations only evolved in the strains of the first replicate of the experiment,
192 but across most of them (22 out of 27 sequenced strains), and across all treatments, including
193 the control. Within the 1st replicate of the experiment, the presence of this SNP in *tpbB* did not
194 explain MIC fold-change towards any of the tested antimicrobials (Fig. S8 and Table S3).
195 On the other hand, SNPs in the *oprL* gene, a membrane lipoprotein which plays an important role
196 in the interaction of *P. aeruginosa* with the environment (42), evolved only in strains of the second
197 replicate of the experiment. SNPs in *tpbB*, in the *orpL* gene they were found in most strains (20
198 out of 27), and across all treatments including the control. Unlike *tpbB*, however, SNPs found in
199 *oprL* (leucine replaced by a phenylalanine in position 43) are predicted to impair protein function.
200 Thus, the presence of this SNP increased MIC fold-change towards Melittin, Pexiganan and
201 Cecropin P1 (Fig. S9 and Table S3).
202 LasR is a transcriptional regulator that controls the expression of virulence factors and biofilm
203 formation in *P. aeruginosa* (43). In our experiments, we found a high number of different SNPs in
204 the *lasR* gene, for most selection regimes, accounting for 27 different SNPs across 29 strains.
205 SNPs in *lasR* were also present in 3 out of the 6 control strains. Among these 27 different SNPs,
206 only 6 were deemed not to affect protein function by Provean, whereas the rest were deleterious.
207 Despite this feature, the presence, or absence, of SNPs in the *lasR* gene is not associated with
208 fold-changes in MIC towards any of the tested antimicrobials (Fig. S10 and Table S3).
209 We also found SNPs in several members of the *wbp* pathway leading to the synthesis of the B-
210 band O-antigen of the Lipopolysaccharide (LPS) in *P. aeruginosa* (44). The most commonly found
211 SNP was a frameshift variant of *wbpA,* while the second most commonly found was a missense
212 mutation in *wbpA*, leading to the replacement of a valine in position 32 by a glycine. The 3 SNPs
213 found in *wbpL* also caused frameshifts, as did the 4 SNPs present in the *wbpI* gene. According to
214 Provean, all these SNPs were deleterious, thus inactivating the products of the respective genes.
215 It has been shown that any missing member of this pathway led to a loss of the B-band O-Antigen
216 of LPS in *P. aeruginosa* (45). Since, *wbp* SNPs found herein were deemed deleterious, we
217 consider these together as inactivating the *wbp* pathway (named "*wbp* genes" in the figures; Fig.
218 S11). Nonetheless, we did not find these deleterious SNPs to affect MIC fold-change towards any
219 of the tested antimicrobials (Fig. S11 and Table S3). Additionally, given that such SNPs were

220 present in all treatments, including the control, once again indicates that they were unlikely to
221 have been selected by our antimicrobials.
222 Among the 5 majorly found gene mutations, only *phoQ* did not show any SNPs in the control
223 group. The *phoQ* gene codes for a Mg^{2+} sensor which is part of a two-component system that
224 controls several pathogenic properties in Gram-negative bacteria (46). In our experiments, the
225 most represented SNP in *phoQ* (in 28 strains out of 29) leads to a replacement of a valine in
226 position 260 by a glycine, which was previously associated to colistin resistance in *P. aeruginosa*
227 isolates (47). All SNPs were deemed deleterious by Provean.
228 The *phoQ* gene mutation was, in fact, the most frequently observed mutation (present in 29
229 different strains), although its distribution was not consistent throughout all the evolved strains.
230 While SNPs were present in all the strains evolved in the presence of PA13, SLM1 and p-FdK5
231 20/80, in 4 out of 6 of the p-FdK5 and FK20-selected strains and in 3 out of 6 of Pexiganan-
232 selected strains, they were absent from Melittin and Cecropin P1-selected strains, as well as the
233 control strains. Moreover, the presence of this SNP in *phoQ* is associated to a higher MIC fold-
234 change towards PA13, SLM1, SLM3, p-FdK5 and p-FdK5 20/80 (Fig. S12 and Table S3).
235 There were only 3 strains in which no SNPs were detected compared to the ancestor PA14: 1 in
236 the Melittin, 1 in the Cecropin P1 and 1 in the control selection regimes (Fig. 3 and S4). However,
237 both the Melittin- and Cecropin P1-evolved strains showed a higher resistance towards Melittin
238 and Cecropin P1 respectively. Moreover, it would have perhaps been expected to find more than
239 just one mutation-less strain in the control group, as it was evolved absent of AMP/RPMs.
240 Nonetheless, naturally occurring mutations result of continuous culturing are expected (48, 49),
241 and, in fact, wild-type PA14 was shown to have a 6.12×10^{-4} spontaneous mutation rate per
242 genome (50).

243 5. <u>The Hill coefficient evolves with the MIC.</u>

244 The steepness of the pharmacodynamic curves (i.e. the Hill coefficient, kappa; κ) generated from
245 time-kill curves provide information about the width of the mutant selection window (i.e the
246 concentration range where resistant mutants are selected for; MSW), as a higher kappa results
247 in a narrower MSW (Fig. 4). Therefore, we analysed kappa evolution for the most resistant strains,
248 in each selection regime, by correlating it with their respective MIC fold-change (Fig. 5). The
249 kappa value of the most resistant evolved strains was normalised to that of the ancestor, for each

AMP/RPM. Six out of eight AMP/RPMs can be found in the lower-right quadrant of MIC fold-change and kappa fold-change correlation (Fig. 5), therefore not only evolving resistance to PA14, but also generating a lower kappa than that of the ancestor strain. Indeed, a Spearman's correlation shows an inverse relationship between MIC and kappa fold-change (ρ= -0.8743; p-value=0.0045), where a lower kappa correlates to a higher MIC, except for p-FdK5-evolved strains.

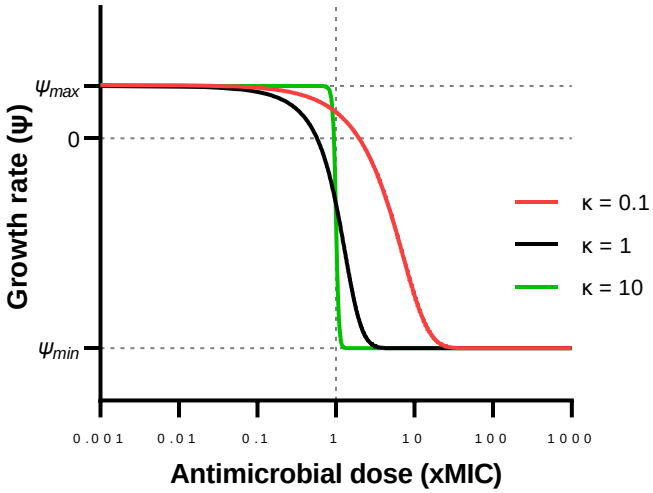

Figure 4 – Schematic illustration of the four parameters predicted by the Hill function: zMIC, ψ_{max}, ψ_{min}, and κ. The zMIC is estimated by the lowest concentration that inhibits the growth of the whole treated bacterium population. While ψ_{max} represents the maximal growth rate of bacteria (i.e. in absence of antimicrobials), ψ_{min} represents the minimal bacterial growth rate, or maximal killing rate of the antimicrobial treatment. The Hill coefficient, κ, predicts the shape and slope of the pharmacodynamic curve; the higher κ is, the steeper the pharmacodynamic curve. Pharmacodynamic curves are represented in different colours (i.e. red, black and green) to portray the change in slope and MIC values.

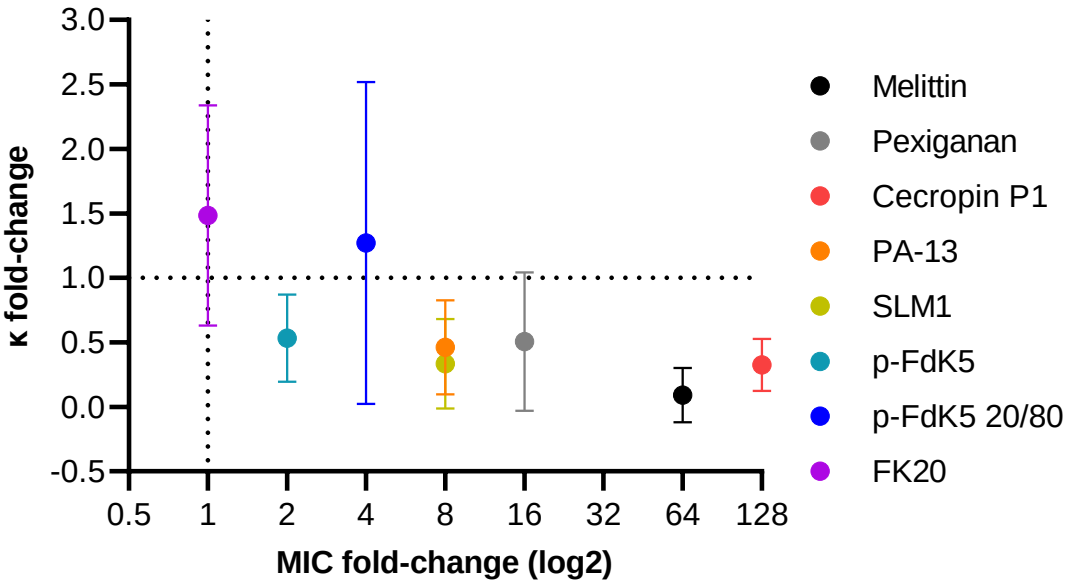

Figure 5 – The MIC and Hill coefficient (κ) of selected strains seem to evolve in correlational fashion. Graphic representing the correlation between evolution of resistance evolution and kappa (ρ=-0,8743; p-value=0,0045). Resistance determined by MIC assay of each strain toward the corresponding peptide, shown as log2 fold-change of the ancestor MICs. Evolution of kappa determined by Hill function-based Rstan model, shown as fold-change of the ancestor's kappa. Each dot represents the mean of triplicates.

Using p-FdK5 20/80, despite evolving resistance, generated a slightly higher κ compared to that of the ancestor strain, therefore maintaining the sensitivity towards the evolved strains. As previously seen (Fig. 1), only under FK20 selection could resistance evolution not be observed, during the 4 weeks under selection, yet it resulted in a higher kappa compared to the that of the ancestor (Fig. 5).

Discussion

The present work was primarily motivated by a growing necessity and interest in exploring novel alternatives to conventional antibiotics. By using a combined approach of experimental evolution, pharmacodynamic modelling and genome re-sequencing, we show how novel random peptide libraries compare to single AMPs in respect to antimicrobial resistance evolution. AMPs have been gaining attention for their potential as antimicrobial agents, partly because of the low probability of resistance evolution (7, 8, 10, 51). In fact, the WHO reported that 15.2% of antibacterials in the preclinical pipeline are AMPs (52), a notable increase from 10.7% reported in the previous review (53). Our hypothesis was that RPMs, as a cocktail of multiple AMPs, would represent an increased set of challenges for bacteria to overcome compared to single AMPs, potentially delaying resistance evolution.

Having selected a broad array of AMPs and RPMs, shown to be active against PA14 *via* MIC determination (Table S1), we saw that resistance evolved against the great majority (2 to 128-fold MIC increase; Fig. 1). These observations are consistent with previous evidence showing that despite lower probability of resistance evolution against AMPs compared to conventional antibiotics, *in vitro* resistance evolution towards AMPs can evolve (13, 54, 55). Conversely, it was observed that random peptide libraries (RPMs), based on cationic and hydrophobic moieties, can significantly delay, or avoid, resistance evolution when compared to single sequence AMPs (Fig. 1 and S5). While palmitic acid-modified RPMs, p-FdK5 and p-FdK5 20/80, were able to greatly reduce the magnitude of resistance evolution, FK20 was the only one effectively escaping it within

299 the context of our experimental setting (Fig. 1). The selection setting herein used covered 4
300 weeks, which is consistent with treatment regimens of *P. aeruginosa* infections (35).
301 Random peptide libraries encase a cocktail of AMPs. Whereas FK20, a 20-mer, can produce over
302 1 million AMP combinations (2^{20}), p-FdK5 and p-FdK5 20/80, although modified with palmitic acid
303 for increased hydrophobicity, being 5-mers, provide less AMP combination possibilities (32 and
304 less, respectively) (21, 22, 26). Hence, the availability of a cocktail of multiple AMPs seems to
305 favour the usage of RPMs, as it creates an increased set of challenges for bacteria to overcome,
306 which can potentially delay resistance evolution. However, drug combinations (including AMPs)
307 should be carefully planned, to avoid the risk of leading to formulations that are inferior to using
308 single agents. Pena-Miller et al. make an interesting case when trying to achieve optimal
309 synergistic effects in drug combinations (56): synergy can exert strong selection for resistance,
310 leading to consistent antagonistic emergence. Thus, unless super-inhibitory doses are applied
311 until the pathogen is successfully cleared, synergistic antibiotics could have the opposite effect
312 and lead to increased pathogen load.
313 Analysis of the cross-resistance/collateral sensitivity results (Fig. 2) revealed some interesting
314 patterns. Cecropin P1-evolved strains show collateral sensitivity to Pexiganan, PA-13 and FK20.
315 Conversely, Pexiganan, PA-13 and FK20-evolved strains show cross-resistance to Cecropin P1.
316 Remarkably, all evolved strains show collateral sensitivity to FK20, which could potentially lead to
317 a positive impact on single AMPs if combined with FK20. In fact, several studies have proposed
318 collateral sensitivity as a promising strategy to slow down the resistance evolution process and
319 even reverse the pre-existing resistance (39, 57-59). Imamovic and collaborators demonstrated
320 that resistance evolution to *P. aeruginosa* for antibiotics used in cystic fibrosis patients caused
321 collateral sensitivity to other antibiotics (39). The study showed that the optimized drug treatment,
322 based on the collateral sensitivity interactions, effectively eradicated the resistant subpopulation
323 from the patient's lungs.
324 In line with previous studies, growth parameters lag time and maximum growth rate (Vmax) were
325 used to estimate cost of resistance evolution (14, 60). Our investigation revealed that strains
326 evolved in the presence of Pexiganan, PA-13, SLM3 and FK20 displayed a fitness cost, resulting
327 in significantly increased lag times compared to control (Fig. S1-A). This result is surprising in the
328 case of FK20-evolved strains, which did not evolve resistance. There were no differences

329 between the lag time of the ancestor and the procedural controls after selection (Fig. S1-A), thus
330 adaptation to the experimental conditions did not affect this aspect of the bacterial fitness. Ward
331 and associates (61) have shown that, clinically isolated MDR strains of *P. aeruginosa* frequently
332 have similar fitness in the absence of antibiotics. Therefore, under certain circumstances, using
333 AMP formulations against which resistance evolution is more costly, might be more effective in
334 preventing resistance evolution, though the relationship between cost and resistance is not
335 always strong (62).
336 No selection regime significantly affected Vmax compared to control, however, the Vmax of the
337 control groups was higher than that of the ancestor (Fig. S1-B). Faster growth rates than that of
338 the ancestor strain have been shown to result from adaptation to a serial passaging environment
339 (63, 64), due to an enhanced ability to acquire, or more efficiently utilize available nutrients during
340 post-exponential growth. On the other hand, no significant differences in Vmax were found
341 between experimentally evolved strains, in either treated or control regimes (Fig. S1-B). A study
342 that induced bacterial resistance to Tachyplesin I (including in *P. aeruginosa*) similarly revealed
343 that resistance acquisition did not markedly affect Vmax, in comparison to the control, but did
344 extend the lag phase (65). The authors argue that AMP resistance might compromise bacterial
345 fitness in different ways, not necessarily affecting the maximum growth rate.
346 We further studied which mutations evolved in our experimental selection treatments. By finding
347 new mutations that emerge in parallel, independently propagated lines of bacterial strains
348 exposed to antibiotics in controlled environments, are likely the cause of new heritable resistant
349 genotypes (66). Among the five genes comprising most of the SNPs in our dataset, *phoQ* was the
350 only one for which SNPs did not evolve in the control lines, suggesting that it evolved as a
351 response to a selection pressure exerted by some of the antimicrobials of our panel. This SNP
352 results in the substitution of a valine by a glycine in position 260 (Histidine kinase A domain),
353 which was deemed to abolish protein function by Provean. This same SNP has also been
354 previously reported to lead to loss-of-function of the PhoQ protein, leading to an increased
355 resistance to colistin in *P. aeruginosa* by Lee and Ko (47).
356 In *P. aeruginosa*, adaptive resistance to cationic AMPs is known to occur in response to limiting
357 extracellular concentrations of Mg^{2+} and Ca^{2+} cations (67, 68). This adaptation is controlled by
358 two-component regulators PhoP-PhoQ and PmrA-PmrB which upregulate the expression of the

359 *arnBCADTEF* lipopolysaccharide (LPS) modification operon (68). The products of these *arn*
360 genes lead to reducing the net negative charge of LPS, limiting the interaction and self-promoted
361 uptake of polycationic antibiotics (e.g. AMPs and aminoglycosides). *PhoQ* expression allows for
362 the integration of environmental cues when bacterial density is high and nutritional resources are
363 rarefied (69). Inactivation of *phoQ* ultimately lead to constitutive LPS modifications which have
364 been shown to confer *P. aeruginosa* colistin resistance (70).
365 *PhoQ* SNPs were present in all evolved treatments, except Melittin and Cecropin P1-selected
366 strains. Moreover, the presence of this SNP in *phoQ* is associated to a higher MIC fold-change
367 towards PA13, SLM1, SLM3, p-FdK5 and p-FdK5 20/80 (Fig. S12). Interestingly, given that *phoQ*
368 SNPs were not found in Melittin and Cecropin P1-evolved strains, the only antimicrobial-selected
369 group with the *phoQ* mutation, which was not associated with higher MIC fold-change is FK20.
370 Therefore, FK20 is the only selection regime in which the presence of this SNP in the *phoQ* gene
371 was not associated to a higher MIC fold-change.
372 SNPs found in the 4 other genes (*lasR*, *wbp*- genes, *tpbB* abd *oprL*) were also detected in the
373 strains of the control selection regime, which means that antimicrobials are unlikely to have
374 selected for their emergence in our bacterial strains.
375 We found a high number of different SNPs in the *lasR* gene (mostly predicted to be deleterious)
376 in the bacterial strains, although the presence of these SNPs did not affect MIC fold-change
377 towards any of the tested antimicrobials in our experimental setting (Fig. S10). LasR has been
378 shown to play an important role in resistance evolution as part of P. aeruginosa quorum sensing
379 (QS) (71). The *P. aeruginosa* QS circuitry is comprised of at least two complete systems, LasR–
380 LasI and RhlR–RhlI (72). Here, the transcriptional regulator LasR controls the expression of
381 virulence factors, such as elastase LasB17, exotoxin A, pyocyanin and EPS, important players
382 for resistance evolution in *P. aeruginosa* (73). Notably, polymorphic populations of *P. aeruginosa*
383 comprising various mutants for *lasR* are selected first in patients with chronic obstructive
384 pulmonary disease (74). Yet, despite this crucial involvement in resistance, accumulation of SNPs
385 in the *lasR* gene have been shown to be widespread in *P. aeruginosa* isolated from various
386 environments, and in the absence of a distinct selection pressure (75). These previous findings
387 are confirmed in our present study. Interestingly, however, SNPs in *lasR* were absent from strains

388 evolved in the presence of PA13 and FK20, which might indicate a constraint on quorum sensing
389 function imposed by these 2 antimicrobials during evolution.
390 The biosynthesis of the B-band O-antigen of LPS is product of genes in the *wbp* pathway, among
391 which are *wbpA*, *wbpI* and *wbpL* (76). The loss of one gene product in this pathway leads to loss-
392 of-function of the B-band O-antigen at the cell surface (45). We found all SNPs in *wbpA*, *wbpI* and
393 *wbpL* (named "*wbp* genes") to be deleterious, thus it is likely that in our experiments the bacterial
394 strains presenting such a SNP do not possess the B-band O-antigen of LPS. This molecule has
395 been shown to play a critical role in host colonization, providing resistance to both serum
396 sensitivity and phagocytosis (77-79), whereas mutants of *P. aeruginosa* deficient in O-antigen
397 synthesis, are sensitive to the killing effects of human serum-mediated lysis (80).
398 With the emergence of mucoid *P. aeruginosa* within the lungs of CF patients, there are cell surface
399 changes with respect to LPS phenotype, characterized by minor expression or complete lack of
400 B-band O-antigen, while the level of A-band is maintained (78). Once *P. aeruginosa* has colonized
401 the lungs, these LPS modifications are probably beneficial for evasion of host defences (A band
402 is less immunogenic) and for alteration of susceptibility to antibiotics, since loss of B-band O-
403 antigen confers resistance to aminoglycosides (81). Thus, given that we found *wbp* pathway
404 SNPs in every evolved treatment, including the control, and that they do not explain MIC fold-
405 change, one could propose that these gene mutations resulted from an adaptation to a biofilm
406 environment, rather than from selection by the panel of antimicrobials tested.
407 We found a SNP in the tpbB gene (also called yfiN), coding for a diguanylate cyclase which
408 regulates the output of messenger cyclic-di-GMP (c-di-GMP) (82), in only 1 of the 2 experimental
409 blocks. (Fig. S8). Several *Pseudomonas* strains (including PA14) undergo phenotypic
410 diversification while adapting to the biofilm environment, forming small colony variants (SCVs)
411 (82). Strong evidence has linked SCVs formation to elevated levels of messenger cyclic-di-GMP
412 (c-di-GMP), associated with sessile phenotypes, expressing biofilm formation and attachment
413 factors (83). Resistant *P. aeruginosa* SCVs phenotype have been shown to inactivate *yfiR* and
414 *tpbA*, negative regulators of *tpbB*, leading to increased biofilm production (84). In our
415 experimentally evolved strains, the SNP in *tpbB* was found to be neutral, which might explain why
416 no effect of this SNP on the MIC-fold change was detected towards any of the tested
417 antimicrobials (Fig. S8).

418 SNPs in the *oprL* gene were also present in all selection regimes, but only in the second replicate
419 of the experiment. They consist of a leucine substitution by a phenylalanine in position 43, leading
420 to protein inactivation. OprL is the second most abundant outer membrane protein in *P.*
421 *aeruginosa*, equivalent of the *E. coli* peptidoglycan-associated lipoprotein (85). Together with
422 small lipoprotein OprI, OprL interacts with peptidoglycans, maintaining cell integrity (85), offering
423 protection from oxidative stress (86), and contributing to antibiotic resistance mechanisms in *P.*
424 *aeruginosa* by adjusting membrane permeability and multidrug efflux pumps, which secrete the
425 drugs directly out of the cell (87). In the experimentally evolved strains of this study, the presence
426 of this deleterious SNP in the *oprL* gene correlated with a higher MIC fold-change towards Melittin-
427 , Pexiganan- and Cecropin P1- evolved strains (Fig. S9).
428 Altogether, our data points to the efficiency of FK20 to slow down, or prevent, the magnitude of
429 resistance evolution of *P. aeruginosa*. A rationale to consider is that FK20 is a random peptide
430 library of over 1 million sequences, making it very difficult to evolve resistance and hence
431 resistance evolution against FK20 was not discovered within the four-week selection time span
432 in our experiment. In fact, the goal of using multiple antimicrobials would be to achieve a combined
433 effect, leading to killing efficacy and/or resistance avoidance, superior to the sum of their individual
434 counterparts (i.e. synergistic interaction) (37). Synergy between AMPs is common, leading to
435 increased killing efficacy, while constraining resistance evolution, which could explain their
436 combinational occurrence in nature (6, 88, 89). The molecular mechanisms of interactions of
437 AMPs are still largely unknown (6), although it has been suggested that synergism resulting of
438 combined AMPs can form a “supermolecule” and more stable pores (90). Furthermore, pore-
439 forming peptides can also assist other coapplied transmembrane AMPs to quickly invade bacterial
440 cells and substantially interrupt the metabolism (91).
441 Insight on why antimicrobial resistance against AMPs evolves with low probabilities, or in the case
442 of FK20 with extremely low probabilities, relies on the molecular mechanisms of killing, but also
443 on the investigation of pharmacodynamics *in vitro*, such as the one portrayed herein and by others
444 (6, 92) and *in vivo* (93). Our study revealed that AMP resistance evolution in *P. aeruginosa*
445 resulted in increased MICs, except for FK20, but also that the Hill coefficient, kappa, evolves as
446 well (36). Kappa (κ) describes how sensitive the bacterial populations net growth rate is to
447 changes in antimicrobial concentration. High κ values represent steeper pharmacodynamic

448 curves (i.e. for concentrations close to the MIC, a small increase in concentration leads to a big
449 decrease in net growth). Therefore, for high κ values a given antibiotic substance (e.g. random
450 peptide libraries or AMP combinations) has a narrower range of concentrations exerting selection
451 on resistant bacteria over susceptible ones (6, 37). This leads to the idea that kappa might relate
452 to the probability of resistance evolution against AMPs (12).
453 A negative correlation between MIC fold-change and kappa fold-change revealed that, generally,
454 lower resistance evolution led to steeper pharmacodynamic curves (i.e. kappa; Fig. 6). Similarly,
455 El Shazely et al. have previously shown a proof-of-concept study illustrating that kappa evolves
456 in *S. aureus* (92). How kappa and the actual AMP-membrane interactions are related in our
457 examples, and in fact in most, requires further study. Work by Srinivasan et al. has studied and
458 summarized possible mechanisms including cooperativity, oligomerization and aggregation of
459 AMP molecules (94).
460 Yu and colleagues have shown that MIC and kappa significantly varied between single AMPs and
461 AMP combinations (6). As numbers of AMPs increased in combination, the MIC of the
462 combinations decreased and, reversibly, kappa increased. Random peptide libraries are
463 combinations of multiple random AMP sequences, a feature that might be crucial and hold
464 potential for outperforming combinations of a few single AMPs.
465 The mutant selection window (MSW) is defined as the range of antimicrobial concentrations
466 where the resistant mutants are selectively favoured over susceptible strains (95). The upper
467 bound is given by the MIC of the resistant mutant, the lower bound, also known as the minimal
468 selective concentration (96), is reached when the net growth rates of the resistant and susceptible
469 strains are equal. By using random peptide libraries, such as FK20, that lead to higher kappa
470 values, in comparison to single AMP-evolved strains, could narrow the range of concentrations
471 selecting resistance (i.e. the MSW).
472
473 **Conclusions**
474 This work reinforced the idea of combinational therapy as a path for tackling antibiotic resistance,
475 highlighting the potential therapeutical capacity of random peptide libraries. Herein, a 20-mer
476 random peptide library, FK20, was shown to avoid resistance and remain sensitive after selection,
477 despite evolving mutations and fitness costs. Our findings suggest that *P. aeruginosa* detects the

478 presence of these antimicrobial agents, but for the duration of our *in vitro* selection protocol (i.e.
479 four weeks), were not able to evolve effective resistance mechanisms. Additionally, these cationic
480 and hydrophobic AMP cocktails can be synthesized affordably and have shown to be non-toxic
481 and non-haemolytic in a mouse model (21, 22).The findings herein depicted strengthen the case
482 for favouring the usage of random cocktails of AMPs over single AMPs, against which resistance
483 evolved *in vitro*.
484 In the past, promising studies have claimed novel antibiotics "resistance-proof", able to stay
485 effective at killing their target pathogens, such as the case of Teixobactin (97), being later refuted
486 (98). Thus, despite the positive findings herein evidenced for FK20, one should side with caution.
487 Moreover, further studies should be conducted concerning the interaction of these RPMs with the
488 host innate immunity. The usage of AMPs/RPMs that strongly synergize with host innate immune
489 response should be favoured, as it could lead to an overall reduction in dosage, hence reducing
490 potential side effects (99). A synergistic strategy involving random peptide libraries and the host
491 immune response holds potential to be a cost-efficient way to reduce bacterial loads and avoid
492 resistance evolution.
493
494 **Materials & Methods**
495 Bacterial strains and growth conditions
496 All experiments were performed with the *P. aeruginosa* 14 strain (PA14; kindly provided by Yael
497 Helman) (100). This strain is defined as the ancestor strain. Prior to each experiment, strains were
498 plated on Mueller-Hinton (MH) agar plates (HiMedia), and individual colonies were picked and
499 grown in MH broth overnight at 37°C. All bacterial cells used in this study were stored in 25%
500 glycerol at -80°C.
501 Synthesis of antimicrobial peptides
502 Six different AMPs and three RPMs were selected for experimental evolution (Table S1). In
503 addition to the peptides developed in house (i.e. SLM1, SLM3, p-FdK5, p-FdK5 20/80 and FK20;
504 (22, 25, 26)), four additional AMPs were selected. Melittin is the major protein component of the
505 venom of the European honeybee (*Apis mellifera*) (101). Pexiganan is a synthetic analog of
506 magainin peptides, isolated from the skin of the African clawed frog (102). Cecropin P1 was the
507 first found mammalian cecropin, isolated from pig small intestine (103), presenting extensive

508 homology to earlier discovered insect cecropins (104). PA-13 is a short synthetic a-helical hybrid
509 peptide, inspired by cathelicidin and aurein (105). While SLM1 and SLM3 are specific palmitic
510 acid-modified 5-mer peptides, composed of L-Lysine and/or L-Phenylalanine, part of a 32-peptide
511 library, p-FdK5 and p-FdK5 20/80 are randomized 5-mers, using L-Phenylalanine and D-Lysine
512 (to the ratios of 1:1 and 1:4, respectively; Fig. S1) (25, 26). Lastly, FK20 was synthetized as
513 random peptide of L-Phenylalanine and L-Lysine (1:1 ratio) (22).
514 All peptides were synthesized by 9-fluorenylmethoxy carbonyl (Fmoc) solid-phase peptide
515 synthesis (SPPS), using a peptide synthesizer (Liberty Blue; CEM, USA). To generate lipo-RPMs
516 and SLMs, acylation was produced by bounding palmitic acid to the N-terminus of the desired
517 peptide/RPM, using the same Fmoc chemistry, albeit that overnight shaking, at room temperature,
518 was used instead of microwave irradiation (26). Upon synthesis completion, peptides were,
519 sequentially, cleaved from the resin (95% trifluoroacetic acid [TFA], 2.5% water, and 2.5%
520 triisopropylsilane [TIPS]), resuspended in double distilled water (DDW), frozen and lyophilized.
521 The resulting crude peptide was dissolved in dimethyl sulfoxide (DMSO) and purified by
522 semipreparative reversed-phase high-performance liquid chromatography (RP-HPLC), while
523 matrix-assisted laser desorption ionization–time of flight mass spectrometry (MALDI-TOF-MS)
524 was utilized for verification of the peptide mass and purity. RPMs containing phenylalanine and
525 lysine (FK20, pFdK5, pFdK5 20/80) were synthesized as previously described (21).
526 Minimum Inhibition Concentration (MIC) determination
527 MIC values were determined following a standard serial dilution protocol, as described elsewhere
528 (27). Briefly, PA14 cells were grown overnight in MH broth, at 37°C and 200 rpm. Subsequently,
529 cells were diluted 1:100 in MH broth and grown until reaching an optical density at 595 nm (OD_{595})
530 of 0.1. Then, 100 µL of 5×10^5 CFU/mL were inoculated into each well in 96-well plates that
531 contained a serial dilution of AMPs or RPMs. Each plate contained 3 replicate lines per peptide.
532 The MICs were defined as the lowest concentration at which there was inhibition of bacterial
533 growth by at least 90%, after 24h, by measuring the OD_{595}.
534 The MIC was determined on 3 occasions: 1) prior to the experiment, to determine the
535 concentration of our focal peptides to be used at the start of the experimental evolution (i.e. MIC
536 of the ancestor strain); 2) at the end of the experimental evolution, detect an increase, or
537 decrease, in the resistance of the experimentally evolved strains to our peptides of interest; 3) to

538 evaluate whether the experimental evolution of a certain treatment was accompanied by an
539 increase, or decrease, in resistance or sensitivity to another antimicrobial (i.e. cross-resistance or
540 collateral-sensitivity).
541 For time containment reasons, the design of the cross-resistance/collateral sensitivity
542 experiments are not full factorial, instead, we focussed on comparisons we found most relevant:
543 1) we exposed strains evolved in the presence of the AMPs Melittin, Pexiganan, Cecropin P1 and
544 PA13, and the RPM FK20 to each other; 2) we then exposed strains evolved in the presence of
545 palmitic acid-modified peptides to peptides of the same family, namely SLM1-, SLM3- and p-
546 FdK5-evolved strains to SLM1, SLM3, p-FdK5 and p-FdK5 20/80.
547 The MIC of evolved strains was divided by MIC of the ancestor to determine the respective fold-
548 change in comparison to the ancestor (see “Statistical Analysis” section).
549 Experimental evolution procedure
550 Prior to evolution with AMPs/RPMs, a PA14 colony was transferred from an MH agar plate into
551 5 mL MH broth in a 50 mL tube and incubated overnight, at 37°C and 200 rpm. Subsequently, this
552 starter culture was diluted 20-fold into a 1.5mL Eppendorf tube containing 850 µL MH broth, to
553 maintain the same headspace ratio of 96-well plates, used in the experimental evolution
554 procedure, and incubated, overnight, under the same conditions (37°C and 200 rpm). This
555 process was repeated for 7 transfers to adapt the bacteria to the experimental conditions.
556 The experimental evolution procedure was designed to exert selective pressure while avoiding
557 extinction of bacterial lines, as previously described (27). Each line was exposed to 4
558 concentrations of AMP/RPMs, according to their MIC, as follows: 1.5x, 1x, 0.5x, and 0.25x (Table
559 S1). Experiments were performed in 96-well plates, and each AMP/RPM had 3 parallel replicates
560 (sharing the same ancestral inoculum). Each plate included 8 wells with bacteria absent of
561 AMPs/RPMs, as a positive control, as well as 4 wells with just medium, as negative control. Daily,
562 10 µL of the previous plate was transferred into 190 µL of fresh medium and AMPs. Every 4 days,
563 bacteria from the highest concentration of AMP/RPM were selected and transferred into 4
564 concentrations in the new plate. MIC was doubled when growth was observed in 4 out of 6 lines
565 at the MIC or higher. The experimental evolution was carried out for 27 transfers (approx. 114
566 generations). Before every selection or MIC increment, samples were taken for fossil record in
567 25% glycerol stocks and preserved at -80°C to avoid line extinction. Spot plating was performed

568 on MH agar, containing 5 µg/mL tetracycline, to confirm growth before selection. Experimental
569 evolutions were performed twice, yielding 6 replicates per selection regime over 2 replicates of
570 the experiment.

571 Fitness cost of evolved strains

572 Bacterial cells were grown overnight in MH broth and then diluted to an OD_{595} of 0.1. For each
573 strain, 200µL of culture were transferred into 96-well plates, with 3 technical replicates. Optical
574 density (OD595) was measured every 15 min for 24 h using an Epoch 2 microplate reader
575 (BioTek). Lag time and Vmax were assessed using the plate reader software (Gen5). The values
576 measured in the experimentally evolved strains were divided by the values of their respective
577 ancestors and expressed as lag time fold-change and Vmax fold-change (see 'Statistical Analysis'
578 section).

579 DNA Isolation

580 Genomic DNA for whole genome sequencing was isolated using GeneMATRIX Bacterial and
581 Yeast genomic DNA purification kit (Roboklon, Germany) following manufacturer's instructions.
582 Four µl of 10 mg/ml freshly prepared lysozyme and lysostaphin (both from Sigma) each were
583 added into bacterial lysate. The DNA quantity and quality were estimated by measuring the optical
584 density at A260/280 using the Nanodrop spectrophotometer (Thermo Scientific) and the Qubit™
585 4 Fluorometer (Thermo Scientific).

586 Sequencing

587 At the end of each replicate of the experimental evolution experiment, 10 µL of the content of
588 each well was plated on MH agar and incubated overnight. One single colony was picked per
589 plate/well to be re-sequenced. As a reference genome, we used a *de novo* assembly of a single
590 colony of PA14 taken from our frozen stock (after overnight culture).

591 The library of the ancestor strain was sequenced on a minion (Oxford Nanopore Technologies,
592 Oxford), at 400 bps translocation speed, using a kit 14 chemistry flowcell, and the resulting raw
593 sequencing data were basecalled using Guppy model dna_r10.4.1_e8.2_400bps_sup.
594 Sequencing reads were adaptor trimmed using porechop (106) and filtered using filtlong (107) to
595 retain approximately 150-fold coverage comprising reads of at least 1000 bp. The filtered reads
596 were assembled using flye (108), which produced a single circular contig that was further polished
597 using medaka consensus (109). The remaining errors were corrected using illumina reads

598 together with polypolish (110). Finally, the start position of the assembly was adjusted to begin at
599 dnaA using circlator (111). The result was annotated with prokka (112).
600 Endpoint re-sequencing of the evolved strains was done on an Illumina HiSeq2000 with 100bp
601 paired-end reads (Wellcome Trust Centre for Human Genetics, Oxford, UK). The sequencing data
602 had a mean depth of 35.9x and a mean coverage of 76.4% at 30x depth. Sequencing Adaptors
603 were trimmed with trimmomatic (113). Snippy (114) was used to call variants using by default
604 parameters, with the annotated assembly described above as a reference sequence. The
605 Provean software tool was used to predict the effect of SNPs on the function of their target protein,
606 namely amino acid substitution or indels (40).
607 Killing Curves
608 AMP/RPM-selected strains were serially diluted (two-fold concentration gradient), starting from
609 10x MIC, in 96-well plates. Approximately, 2–3x10^6 log-phase bacteria were added to a total
610 volume of 100 ml. The plates were incubated at 37°C. As it is known that AMP-mediated killing is
611 quick (115, 116), dose-response was monitored within 60 min (6). To do so, 10 μL of bacterial
612 suspension were sampled after 5, 10, 20, 40 and 60 min., then immediately diluted in 90μL PBS
613 and plated on square solid MHA plates. These solid agar plates were transferred into a 37°C
614 incubator and incubated for 24h before counting CFUs. The same procedure was followed to
615 assess killing curves for the sensitive ancestor PA14 strain. The assays were performed in
616 triplicates.
617 Modelling killing curves – Pharmacodynamics
618 Pharmacodynamics capture the functional relationship between drug dosage and bacterial growth
619 or death. To model the killing curve, discribing the relationship between the concentration of
620 AMPs/RPMs and the killing and/or growth rate of the exposed bacteria, the Hill function was used
621 (36). This function estimates four parameters: zMIC, κ, ψ_{min}, and ψ_{max} (Fig. 4). The zMIC is the
622 MIC estimated by fitting; κ, the Hill coefficient, depicts the steepness of the curve relating bacterial
623 growth to drug concentration; ψ_{min}, and ψ_{max} represent the minimum and maximum growth rates
624 of bacteria, respectively (see Hill function equations in supplementary methods). Growth rate and
625 killing rate of bacteria are estimated from the time-kill curves as the change of CFU over time by
626 using generalized linear regression. The data for CFU were all log transformed. The starting point
627 of linear regression was the first measurement. We then fitted the growth rate and killing rate with

628 equation 4 (see supplementary methods), based on the Markov chain Monte Carlo (MCMC)
629 method and generated the pharmacodynamic curves. Pharmacodynamic parameters of the most
630 resistant experimentally evolved strains and ancestor were estimated and a summary can be
631 found in Table S2.

632 Statistical analysis

633 All the data was analysed using the R software (117) and figures were produced using GraphPad
634 Prism, version 9 for Windows, GraphPad Software, Boston, Massachusetts USA.

635 We normalized the MICs of the different evolved strains generated in this series of experiments
636 (as well as the control strain) by dividing them with the MIC of their respective ancestors, which
637 represents the MICs before applying the selection regime. The resulting variable is a fold-change
638 in MIC ("MIC fold-change") at the end of the experimental evolution compared to the beginning.

639 Similarly, we normalized both fitness readouts duration of the lag phase (lag time) and maximum
640 slope of the bacterial growth curve (Vmax) to the readouts of the ancestor of the given evolved
641 strain by dividing the values of the evolved strains to that of their respective ancestors. The
642 resulting variable is a fold-change in Vmax and lag time during experimental evolution: Vmax fold-
643 change and lag time fold-change.

644 These response variables are therefore ratios, which are non-integer despite representing count
645 data. They showed the dispersion typical of count data, as well as a heterogeneity in the variances
646 between treatments. MIC fold-changes had a maximum of 3 digits after the comma. They were
647 multiplied by 1000 to analyse them with models fitted for a negative binomial distribution (see
648 details below), since this distribution assumes a positive and integer response variable. We
649 multiplied the lag time fold-change by 100 and rounded it up according to the value of the third
650 digit after the comma to perform a similar analysis. However, such was not the case for the Vmax
651 fold-change data which satisfied the assumptions of a Linear Mixed Model and did not require to
652 be multiplied and rounded.

653 We then analysed the MIC and lag time fold-change of single sequence AMPs and RPMs strains,
654 generated by experimental evolution, with a Generalised Linear Mixed-Effect Model (GLMM),
655 fitted for a negative binomial distribution, according to the selection regime. Since the MIC fold-
656 change was always assessed towards the antimicrobial used, as a selection pressure during
657 experimental evolution, there was no further need to include the antimicrobial towards which the

658 MIC was measured with as an explanatory variable. Since the whole experiment was replicated
659 in 2 experimental blocks, we included this experimental block as a random factor. We used the
660 'glmmTMB' function of th 'glmmTMB' package (118). As stated above, we analysed the Vmax
661 fold-change of the resulting strains with a Linear Mixed effect Model (LMM, 'lmer' function of the
662 'lme4' package) (119), including Vmax fold-change as a response variable according to the
663 selection regime and the experimental block as a random factor.
664 Pairwise comparisons between selection regimes can be performed by eye, as previously
665 reported (120, 121): the difference between two selection regimes is deemed significant when the
666 95% confidence intervals (95CI) do not overlap more than half of their length. Effect plots for post-
667 hoc comparison between different selection regimes (estimates of the models with the
668 corresponding 95CIs) are displayed in the Supplementary Material figures S5 to S7, which were
669 generated with the 'effects' package (122, 123).
670 We next used the cross-resistance/collateral sensitivity dataset to analyse whether the presence,
671 or absence, of SNPs in the 5 genes which concentrated most of the SNPs (*lasR*, *wbp* genes,
672 *phoQ*, *tpbB* and *oprL*) affected the MIC fold-changes in the bacterial strains. We built the following
673 model for each gene/antimicrobial combination: MIC fold-change x1000 as a response variable
674 explained by presence/absence of SNP in a gene, and the experimental block as a random factor
675 ('glmmTMB' function of the 'glmmTMB' package). Since SNPs in *tpbB* and *oprL* only emerged in
676 strains from 1 of the 2 experimental blocks, we performed this analysis only in the replicate in
677 which SNPs were present, using the 'glm.nb' function of the 'MASS' package (124). We
678 considered all bacterial strains, regardless of their selection regime of origin, since the selection
679 regime, which affects the presence, or absence, of SNPs in the strains, would have been colinear
680 with the latter.
681 Correlation between kappa fold-change and MIC fold-change was assessed using Spearman's
682 test (ρ), which estimates a rank-based measure of association, through the 'cor.test' function
683 included in the 'stats' package (125).
684 Pharmacodynamics analyses were performed using Rstan (126).
685
686
687

Acknowledgements

The authors thank P.R. Johnston for the assistance in whole-genome sequencing analysis, E. Bittermann for the input and assistance in setting up samples for whole-genome sequencing and Ronan Murphy for critically reading the manuscript and helping with data interpretation.

Funding

This work was funded by the Joint Berlin-Jerusalem Postdoctoral Fellowship Program offered by the Freie Universität Berlin (FUB) and Hebrew University of Jerusalem (HUJI). The project was further supported by a grant from the Volkswagen Foundation (grant no. 96517).

Conflicts of interest

The authors declare no competing interests.

References

1. Antimicrobial Resistance C. Global burden of bacterial antimicrobial resistance in 2019: a systematic analysis. Lancet. 2022;399(10325):629-55.
2. Qiu D, Ke M, Zhang Q, Zhang F, Lu T, Sun L, et al. Response of microbial antibiotic resistance to pesticides: An emerging health threat. Sci Total Environ. 2022;850:158057.
3. Lepore C, Silver L, Theuretzbacher U, Thomas J, Visi D. The small-molecule antibiotics pipeline: 2014-2018. Nat Rev Drug Discov. 2019;18(10):739.
4. Organization WH. The evolving threat of antimicrobial resistance: options for action: World Health Organization; 2012.
5. Czaplewski L, Bax R, Clokie M, Dawson M, Fairhead H, Fischetti VA, et al. Alternatives to antibiotics-a pipeline portfolio review. Lancet Infect Dis. 2016;16(2):239-51.
6. Yu G, Baeder DY, Regoes RR, Rolff J. Combination Effects of Antimicrobial Peptides. Antimicrob Agents Chemother. 2016;60(3):1717-24.
7. Zasloff M. Antimicrobial peptides of multicellular organisms. Nature. 2002;415(6870):389-95.
8. Rathinakumar R, Walkenhorst WF, Wimley WC. Broad-spectrum antimicrobial peptides by rational combinatorial design and high-throughput screening: the importance of interfacial activity. J Am Chem Soc. 2009;131(22):7609-17.
9. Axelsen PH. A chaotic pore model of polypeptide antibiotic action. Biophys J. 2008;94(5):1549-50.
10. Hancock RE. Cationic peptides: effectors in innate immunity and novel antimicrobials. Lancet Infect Dis. 2001;1(3):156-64.
11. Rodriguez-Rojas A, Nath A, El Shazely B, Santi G, Kim JJ, Weise C, et al. Antimicrobial Peptide Induced-Stress Renders Staphylococcus aureus Susceptible to Toxic Nucleoside Analogs. Front Immunol. 2020;11:1686.
12. Yu G, Baeder DY, Regoes RR, Rolff J. Predicting drug resistance evolution: insights from antimicrobial peptides and antibiotics. Proc Biol Sci. 2018;285(1874).
13. Perron GG, Zasloff M, Bell G. Experimental evolution of resistance to an antimicrobial peptide. Proc Biol Sci. 2006;273(1583):251-6.

730 14. Spohn R, Daruka L, Lazar V, Martins A, Vidovics F, Grezal G, et al. Integrated
731 evolutionary analysis reveals antimicrobial peptides with limited resistance. Nat Commun.
732 2019;10(1):4538.
733 15. Bian X, Qu X, Zhang J, Nang SC, Bergen PJ, Tony Zhou Q, et al. Pharmacokinetics and
734 pharmacodynamics of peptide antibiotics. Adv Drug Deliv Rev. 2022;183:114171.
735 16. Liu YY, Wang Y, Walsh TR, Yi LX, Zhang R, Spencer J, et al. Emergence of plasmid-
736 mediated colistin resistance mechanism MCR-1 in animals and human beings in China: a
737 microbiological and molecular biological study. Lancet Infect Dis. 2016;16(2):161-8.
738 17. Tacconelli E, Carrara E, Savoldi A, Harbarth S, Mendelson M, Monnet DL, et al.
739 Discovery, research, and development of new antibiotics: the WHO priority list of antibiotic-
740 resistant bacteria and tuberculosis. Lancet Infect Dis. 2018;18(3):318-27.
741 18. Laxminarayan R, Duse A, Wattal C, Zaidi AK, Wertheim HF, Sumpradit N, et al. Antibiotic
742 resistance-the need for global solutions. Lancet Infect Dis. 2013;13(12):1057-98.
743 19. Tyers M, Wright GD. Drug combinations: a strategy to extend the life of antibiotics in
744 the 21st century. Nat Rev Microbiol. 2019;17(3):141-55.
745 20. Roemhild R, Bollenbach T, Andersson DI. The physiology and genetics of bacterial
746 responses to antibiotic combinations. Nat Rev Microbiol. 2022;20(8):478-90.
747 21. Hayouka Z, Chakraborty S, Liu R, Boersma MD, Weisblum B, Gellman SH. Interplay
748 among subunit identity, subunit proportion, chain length, and stereochemistry in the activity
749 profile of sequence-random peptide mixtures. J Am Chem Soc. 2013;135(32):11748-51.
750 22. Hayouka Z, Bella A, Stern T, Ray S, Jiang H, Grovenor CRM, et al. Binary Encoding of
751 Random Peptide Sequences for Selective and Differential Antimicrobial Mechanisms. Angew
752 Chem Int Ed Engl. 2017;56(28):8099-103.
753 23. Siriwardena TN, Gan BH, Kohler T, van Delden C, Javor S, Reymond JL.
754 Stereorandomization as a Method to Probe Peptide Bioactivity. ACS Cent Sci. 2021;7(1):126-34.
755 24. Stern T, Zelinger E, Hayouka Z. Random peptide mixtures inhibit and eradicate
756 methicillin-resistant Staphylococcus aureus biofilms. Chem Commun (Camb).
757 2016;52(44):7102-5.
758 25. Topman S, Tamir-Ariel D, Bochnic-Tamir H, Stern Bauer T, Shafir S, Burdman S, et al.
759 Random peptide mixtures as new crop protection agents. Microb Biotechnol. 2018;11(6):1027-
760 36.
761 26. Topman-Rakover S, Malach E, Burdman S, Hayouka Z. Antibacterial lipo-random
762 peptide mixtures exhibit high selectivity and synergistic interactions. Chem Commun (Camb).
763 2020;56(80):12053-6.
764 27. Maron B, Rolff J, Friedman J, Hayouka Z. Antimicrobial Peptide Combination Can Hinder
765 Resistance Evolution. Microbiol Spectr. 2022;10(4):e0097322.
766 28. Makovitzki A, Avrahami D, Shai Y. Ultrashort antibacterial and antifungal lipopeptides.
767 Proc Natl Acad Sci U S A. 2006;103(43):15997-6002.
768 29. Makovitzki A, Viterbo A, Brotman Y, Chet I, Shai Y. Inhibition of fungal and bacterial
769 plant pathogens in vitro and in planta with ultrashort cationic lipopeptides. Appl Environ
770 Microbiol. 2007;73(20):6629-36.
771 30. Brotman Y, Makovitzki A, Shai Y, Chet I, Viterbo A. Synthetic ultrashort cationic
772 lipopeptides induce systemic plant defense responses against bacterial and fungal pathogens.
773 Appl Environ Microbiol. 2009;75(16):5373-9.
774 31. Pendleton JN, Gorman SP, Gilmore BF. Clinical relevance of the ESKAPE pathogens.
775 Expert Rev Anti Infect Ther. 2013;11(3):297-308.
776 32. Stover CK, Pham XQ, Erwin AL, Mizoguchi SD, Warrener P, Hickey MJ, et al. Complete
777 genome sequence of Pseudomonas aeruginosa PAO1, an opportunistic pathogen. Nature.
778 2000;406(6799):959-64.
779 33. Livermore DM. Multiple mechanisms of antimicrobial resistance in Pseudomonas
780 aeruginosa: our worst nightmare? Clin Infect Dis. 2002;34(5):634-40.

781 34. Ben Hur D, Kapach G, Wani NA, Kiper E, Ashkenazi M, Smollan G, et al. Antimicrobial
782 Peptides against Multidrug-Resistant Pseudomonas aeruginosa Biofilm from Cystic Fibrosis
783 Patients. J Med Chem. 2022;65(13):9050-62.
784 35. Reynolds D, Kollef M. The Epidemiology and Pathogenesis and Treatment of
785 Pseudomonas aeruginosa Infections: An Update. Drugs. 2021;81(18):2117-31.
786 36. Regoes RR, Wiuff C, Zappala RM, Garner KN, Baquero F, Levin BR. Pharmacodynamic
787 functions: a multiparameter approach to the design of antibiotic treatment regimens.
788 Antimicrob Agents Chemother. 2004;48(10):3670-6.
789 37. Witzany C, Rolff J, Regoes RR, Igler C. The pharmacokinetic-pharmacodynamic
790 modelling framework as a tool to predict drug resistance evolution. Microbiology (Reading).
791 2023;169(7).
792 38. Pál C, Papp B, Lázár V. Collateral sensitivity of antibiotic-resistant microbes. Trends in
793 Microbiology. 2015;23(7):401-7.
794 39. Imamovic L, Sommer MO. Use of collateral sensitivity networks to design drug cycling
795 protocols that avoid resistance development. Sci Transl Med. 2013;5(204):204ra132.
796 40. Choi Y, Sims GE, Murphy S, Miller JR, Chan AP. Predicting the functional effect of amino
797 acid substitutions and indels. PLoS One. 2012;7(10):e46688.
798 41. Ueda A, Wood TK. Connecting quorum sensing, c-di-GMP, pel polysaccharide, and
799 biofilm formation in Pseudomonas aeruginosa through tyrosine phosphatase TpbA (PA3885).
800 PLoS Pathog. 2009;5(6):e1000483.
801 42. Lim A, De Vos D, Brauns M, Mossialos D, Gaballa A, Qing D, et al. Molecular and
802 immunological characterization of OprL, the 18 kDa outer-membrane peptidoglycan-associated
803 lipoprotein (PAL) of Pseudomonas aeruginosa. Microbiology (Reading). 1997;143 (Pt 5):1709-
804 16.
805 43. Gambello MJ, Iglewski BH. Cloning and characterization of the Pseudomonas
806 aeruginosa lasR gene, a transcriptional activator of elastase expression. J Bacteriol.
807 1991;173(9):3000-9.
808 44. Burrows LL, Charter DF, Lam JS. Molecular characterization of the Pseudomonas
809 aeruginosa serotype O5 (PAO1) B-band lipopolysaccharide gene cluster. Mol Microbiol.
810 1996;22(3):481-95.
811 45. Larkin A, Imperiali B. Biosynthesis of UDP-GlcNAc(3NAc)A by WbpB, WbpE, and WbpD:
812 enzymes in the Wbp pathway responsible for O-antigen assembly in Pseudomonas aeruginosa
813 PAO1. Biochemistry. 2009;48(23):5446-55.
814 46. Fields PI, Groisman EA, Heffron F. A Salmonella locus that controls resistance to
815 microbicidal proteins from phagocytic cells. Science. 1989;243(4894):1059-62.
816 47. Lee JY, Ko KS. Mutations and expression of PmrAB and PhoPQ related with colistin
817 resistance in Pseudomonas aeruginosa clinical isolates. Diagn Microbiol Infect Dis.
818 2014;78(3):271-6.
819 48. Heurlier K, Denervaud V, Haenni M, Guy L, Krishnapillai V, Haas D. Quorum-sensing-
820 negative (lasR) mutants of Pseudomonas aeruginosa avoid cell lysis and death. J Bacteriol.
821 2005;187(14):4875-83.
822 49. Perfeito L, Fernandes L, Mota C, Gordo I. Adaptive mutations in bacteria: high rate and
823 small effects. Science. 2007;317(5839):813-5.
824 50. Dettman JR, Sztepanacz JL, Kassen R. The properties of spontaneous mutations in the
825 opportunistic pathogen Pseudomonas aeruginosa. BMC Genomics. 2016;17:27.
826 51. Mookherjee N, Anderson MA, Haagsman HP, Davidson DJ. Antimicrobial host defence
827 peptides: functions and clinical potential. Nat Rev Drug Discov. 2020;19(5):311-32.
828 52. Organization WH. Antibacterial agents in clinical and preclinical development: an
829 overview and analysis. World Health Organization; 2021.
830 53. Organization WH. Antibacterial agents in preclinical development: an open access
831 database. World Health Organization; 2019.

832 54. Dobson AJ, Purves J, Kamysz W, Rolff J. Comparing selection on S. aureus between
833 antimicrobial peptides and common antibiotics. PLoS One. 2013;8(10):e76521.
834 55. Habets MG, Brockhurst MA. Therapeutic antimicrobial peptides may compromise
835 natural immunity. Biol Lett. 2012;8(3):416-8.
836 56. Pena-Miller R, Laehnemann D, Jansen G, Fuentes-Hernandez A, Rosenstiel P,
837 Schulenburg H, et al. When the most potent combination of antibiotics selects for the greatest
838 bacterial load: the smile-frown transition. PLoS Biol. 2013;11(4):e1001540.
839 57. Baym M, Stone LK, Kishony R. Multidrug evolutionary strategies to reverse antibiotic
840 resistance. Science. 2016;351(6268):aad3292.
841 58. Lazar V, Martins A, Spohn R, Daruka L, Grezal G, Fekete G, et al. Antibiotic-resistant
842 bacteria show widespread collateral sensitivity to antimicrobial peptides. Nat Microbiol.
843 2018;3(6):718-31.
844 59. Barbosa C, Beardmore R, Schulenburg H, Jansen G. Antibiotic combination efficacy
845 (ACE) networks for a Pseudomonas aeruginosa model. PLoS Biol. 2018;16(4):e2004356.
846 60. Makarova O, Johnston P, Rodriguez-Rojas A, El Shazely B, Morales JM, Rolff J. Genomics
847 of experimental adaptation of Staphylococcus aureus to a natural combination of insect
848 antimicrobial peptides. Sci Rep. 2018;8(1):15359.
849 61. Ward H, Perron GG, Maclean RC. The cost of multiple drug resistance in Pseudomonas
850 aeruginosa. J Evol Biol. 2009;22(5):997-1003.
851 62. Igler C, Rolff J, Regoes R. Multi-step vs. single-step resistance evolution under different
852 drugs, pharmacokinetics, and treatment regimens. Elife. 2021;10.
853 63. Somerville GA, Chaussee MS, Morgan CI, Fitzgerald JR, Dorward DW, Reitzer LJ, et al.
854 Staphylococcus aureus aconitase inactivation unexpectedly inhibits post-exponential-phase
855 growth and enhances stationary-phase survival. Infect Immun. 2002;70(11):6373-82.
856 64. LaCroix RA, Palsson BO, Feist AM. A Model for Designing Adaptive Laboratory Evolution
857 Experiments. Appl Environ Microbiol. 2017;83(8).
858 65. Hong J, Hu J, Ke F. Experimental Induction of Bacterial Resistance to the Antimicrobial
859 Peptide Tachyplesin I and Investigation of the Resistance Mechanisms. Antimicrob Agents
860 Chemother. 2016;60(10):6067-75.
861 66. Santos-Lopez A, Fritz MJ, Lombardo JB, Burr AHP, Heinrich VA, Marshall CW, et al.
862 Evolved resistance to a novel cationic peptide antibiotic requires high mutation supply. Evol
863 Med Public Health. 2022;10(1):266-76.
864 67. Macfarlane EL, Kwasnicka A, Ochs MM, Hancock RE. PhoP-PhoQ homologues in
865 Pseudomonas aeruginosa regulate expression of the outer-membrane protein OprH and
866 polymyxin B resistance. Mol Microbiol. 1999;34(2):305-16.
867 68. McPhee JB, Lewenza S, Hancock RE. Cationic antimicrobial peptides activate a two-
868 component regulatory system, PmrA-PmrB, that regulates resistance to polymyxin B and
869 cationic antimicrobial peptides in Pseudomonas aeruginosa. Mol Microbiol. 2003;50(1):205-17.
870 69. Groisman EA. The pleiotropic two-component regulatory system PhoP-PhoQ. J
871 Bacteriol. 2001;183(6):1835-42.
872 70. Miller AK, Brannon MK, Stevens L, Johansen HK, Selgrade SE, Miller SI, et al. PhoQ
873 mutations promote lipid A modification and polymyxin resistance of Pseudomonas aeruginosa
874 found in colistin-treated cystic fibrosis patients. Antimicrob Agents Chemother.
875 2011;55(12):5761-9.
876 71. Li Y, Xia L, Chen J, Lian Y, Dandekar AA, Xu F, et al. Resistance elicited by sub-lethal
877 concentrations of ampicillin is partially mediated by quorum sensing in Pseudomonas
878 aeruginosa. Environ Int. 2021;156:106619.
879 72. Gilbert KB, Kim TH, Gupta R, Greenberg EP, Schuster M. Global position analysis of the
880 Pseudomonas aeruginosa quorum-sensing transcription factor LasR. Mol Microbiol.
881 2009;73(6):1072-85.
882 73. Sakuragi Y, Kolter R. Quorum-sensing regulation of the biofilm matrix genes (pel) of
883 Pseudomonas aeruginosa. J Bacteriol. 2007;189(14):5383-6.

884 74. Zhao K, Yang X, Zeng Q, Zhang Y, Li H, Yan C, et al. Evolution of lasR mutants in
885 polymorphic Pseudomonas aeruginosa populations facilitates chronic infection of the lung. Nat
886 Commun. 2023;14(1):5976.
887 75. Ciofu O, Mandsberg LF, Bjarnsholt T, Wassermann T, Hoiby N. Genetic adaptation of
888 Pseudomonas aeruginosa during chronic lung infection of patients with cystic fibrosis: strong
889 and weak mutators with heterogeneous genetic backgrounds emerge in mucA and/or lasR
890 mutants. Microbiology (Reading). 2010;156(Pt 4):1108-19.
891 76. Miller WL, Wenzel CQ, Daniels C, Larocque S, Brisson JR, Lam JS. Biochemical
892 characterization of WbpA, a UDP-N-acetyl-D-glucosamine 6-dehydrogenase involved in O-
893 antigen biosynthesis in Pseudomonas aeruginosa PAO1. J Biol Chem. 2004;279(36):37551-8.
894 77. Hancock RE, Mutharia LM, Chan L, Darveau RP, Speert DP, Pier GB. Pseudomonas
895 aeruginosa isolates from patients with cystic fibrosis: a class of serum-sensitive, nontypable
896 strains deficient in lipopolysaccharide O side chains. Infect Immun. 1983;42(1):170-7.
897 78. Rocchetta HL, Burrows LL, Lam JS. Genetics of O-antigen biosynthesis in Pseudomonas
898 aeruginosa. Microbiol Mol Biol Rev. 1999;63(3):523-53.
899 79. Joiner KA. Studies on the mechanism of bacterial resistance to complement-mediated
900 killing and on the mechanism of action of bactericidal antibody. Curr Top Microbiol Immunol.
901 1985;121:99-133.
902 80. Dasgupta T, de Kievit TR, Masoud H, Altman E, Richards JC, Sadovskaya I, et al.
903 Characterization of lipopolysaccharide-deficient mutants of Pseudomonas aeruginosa derived
904 from serotypes O3, O5, and O6. Infect Immun. 1994;62(3):809-17.
905 81. Kadurugamuwa JL, Lam JS, Beveridge TJ. Interaction of gentamicin with the A band and
906 B band lipopolysaccharides of Pseudomonas aeruginosa and its possible lethal effect.
907 Antimicrob Agents Chemother. 1993;37(4):715-21.
908 82. Wang D, Dorosky RJ, Han CS, Lo CC, Dichosa AE, Chain PS, et al. Adaptation genomics of
909 a small-colony variant in a Pseudomonas chlororaphis 30-84 biofilm. Appl Environ Microbiol.
910 2015;81(3):890-9.
911 83. Malone JG, Jaeger T, Spangler C, Ritz D, Spang A, Arrieumerlou C, et al. YfiBNR mediates
912 cyclic di-GMP dependent small colony variant formation and persistence in Pseudomonas
913 aeruginosa. PLoS Pathog. 2010;6(3):e1000804.
914 84. Pu M, Wood TK. Tyrosine phosphatase TpbA controls rugose colony formation in
915 Pseudomonas aeruginosa by dephosphorylating diguanylate cyclase TpbB. Biochem Biophys
916 Res Commun. 2010;402(2):351-5.
917 85. Remans K, Vercammen K, Bodilis J, Cornelis P. Genome-wide analysis and literature-
918 based survey of lipoproteins in Pseudomonas aeruginosa. Microbiology (Reading). 2010;156(Pt
919 9):2597-607.
920 86. Panmanee W, Gomez F, Witte D, Pancholi V, Britigan BE, Hassett DJ. The peptidoglycan-
921 associated lipoprotein OprL helps protect a Pseudomonas aeruginosa mutant devoid of the
922 transactivator OxyR from hydrogen peroxide-mediated killing during planktonic and biofilm
923 culture. J Bacteriol. 2008;190(10):3658-69.
924 87. Ghazaei C. Antibiotic Resistance Profiles of Pseudomonas aeruginosa Isolates
925 Containing Virulence Genes. Research in Molecular Medicine. 2021;9(4):245-52.
926 88. Marxer M, Vollenweider V, Schmid-Hempel P. Insect antimicrobial peptides act
927 synergistically to inhibit a trypanosome parasite. Philos Trans R Soc Lond B Biol Sci.
928 2016;371(1695).
929 89. Rolff J, Schmid-Hempel P. Perspectives on the evolutionary ecology of arthropod
930 antimicrobial peptides. Philos Trans R Soc Lond B Biol Sci. 2016;371(1695).
931 90. Matsuzaki K, Mitani Y, Akada KY, Murase O, Yoneyama S, Zasloff M, et al. Mechanism of
932 synergism between antimicrobial peptides magainin 2 and PGLa. Biochemistry.
933 1998;37(43):15144-53.
934 91. Brogden KA. Antimicrobial peptides: pore formers or metabolic inhibitors in bacteria?
935 Nat Rev Microbiol. 2005;3(3):238-50.

936 92. El Shazely B, Yu G, Johnston PR, Rolff J. Resistance Evolution Against Antimicrobial
937 Peptides in Staphylococcus aureus Alters Pharmacodynamics Beyond the MIC. Front Microbiol.
938 2020;11:103.
939 93. Zanchi C, Johnston PR, Rolff J. Evolution of defence cocktails: Antimicrobial peptide
940 combinations reduce mortality and persistent infection. Mol Ecol. 2017;26(19):5334-43.
941 94. Srinivasan S, Waghu FH, Idicula-Thomas S, Venkatesh KV. A steady-state modeling
942 approach for simulation of antimicrobial peptide-cell membrane interaction. Biochim Biophys
943 Acta Biomembr. 2020;1862(4):183242.
944 95. Lazzaro BP, Zasloff M, Rolff J. Antimicrobial peptides: Application informed by
945 evolution. Science. 2020;368(6490).
946 96. Gullberg E, Cao S, Berg OG, Ilback C, Sandegren L, Hughes D, et al. Selection of resistant
947 bacteria at very low antibiotic concentrations. PLoS Pathog. 2011;7(7):e1002158.
948 97. Ling LL, Schneider T, Peoples AJ, Spoering AL, Engels I, Conlon BP, et al. A new antibiotic
949 kills pathogens without detectable resistance. Nature. 2015;517(7535):455-9.
950 98. Lloyd DG, Schofield BJ, Goddard MR, Taylor EJ. De Novo Resistance to Arg(10)-
951 Teixobactin Occurs Slowly and Is Costly. Antimicrob Agents Chemother. 2020;65(1).
952 99. Johnston PR, Makarova O, Rolff J. Inducible defenses stay up late: temporal patterns of
953 immune gene expression in Tenebrio molitor. G3 (Bethesda). 2013;4(6):947-55.
954 100. He J, Baldini RL, Deziel E, Saucier M, Zhang Q, Liberati NT, et al. The broad host range
955 pathogen Pseudomonas aeruginosa strain PA14 carries two pathogenicity islands harboring
956 plant and animal virulence genes. Proc Natl Acad Sci U S A. 2004;101(8):2530-5.
957 101. Habermann E, Neumann W. Characterization of the effective components of snake
958 venoms. Naunyn Schmiedebergs Arch Exp Pathol Pharmakol. 1954;223(5):388-98.
959 102. Fuchs PC, Barry AL, Brown SD. In vitro antimicrobial activity of MSI-78, a magainin
960 analog. Antimicrob Agents Chemother. 1998;42(5):1213-6.
961 103. Lee JY, Boman A, Sun CX, Andersson M, Jornvall H, Mutt V, et al. Antibacterial peptides
962 from pig intestine: isolation of a mammalian cecropin. Proc Natl Acad Sci U S A.
963 1989;86(23):9159-62.
964 104. Hultmark D, Steiner H, Rasmuson T, Boman HG. Insect immunity. Purification and
965 properties of three inducible bactericidal proteins from hemolymph of immunized pupae of
966 Hyalophora cecropia. Eur J Biochem. 1980;106(1):7-16.
967 105. Klubthawee N, Adisakwattana P, Hanpithakpong W, Somsri S, Aunpad R. A novel,
968 rationally designed, hybrid antimicrobial peptide, inspired by cathelicidin and aurein, exhibits
969 membrane-active mechanisms against Pseudomonas aeruginosa. Sci Rep. 2020;10(1):9117.
970 106. Wick R. Porechop: adapter trimmer for Oxford Nanopore reads. 2018.
971 107. Wick RR, Menzel P. Filtlong. 2018.
972 108. Kolmogorov M, Yuan J, Lin Y, Pevzner PA. Assembly of long, error-prone reads using
973 repeat graphs. Nat Biotechnol. 2019;37(5):540-6.
974 109. Nanoporetech. Medaka: Sequence correction provided by ONT research. GitHub 2019
975 [Available from: https://github.com/nanoporetech/medaka.
976 110. Wick RR, Holt KE. Polypolish: Short-read polishing of long-read bacterial genome
977 assemblies. PLoS Comput Biol. 2022;18(1):e1009802.
978 111. Hunt M, Silva ND, Otto TD, Parkhill J, Keane JA, Harris SR. Circlator: automated
979 circularization of genome assemblies using long sequencing reads. Genome Biol. 2015;16:294.
980 112. Seemann T. Prokka: rapid prokaryotic genome annotation. Bioinformatics.
981 2014;30(14):2068-9.
982 113. Bolger AM, Lohse M, Usadel B. Trimmomatic: a flexible trimmer for Illumina sequence
983 data. Bioinformatics. 2014;30(15):2114-20.
984 114. Seemann T. Snippy: fast bacterial variant calling from NGS reads. 2015.
985 115. Sochacki KA, Barns KJ, Bucki R, Weisshaar JC. Real-time attack on single Escherichia coli
986 cells by the human antimicrobial peptide LL-37. Proc Natl Acad Sci U S A. 2011;108(16):E77-81.

116. Rangarajan N, Bakshi S, Weisshaar JC. Localized permeabilization of E. coli membranes by the antimicrobial peptide Cecropin A. Biochemistry. 2013;52(38):6584-94.
117. Team RC. R: A language and environment for statistical computing. Vienna, Austria; 2020.
118. Brooks ME, Kristensen K, Van Benthem KJ, Magnusson A, Berg CW, Nielsen A, et al. glmmTMB balances speed and flexibility among packages for zero-inflated generalized linear mixed modeling. The R journal. 2017;9(2):378-400.
119. Bates D, Mächler M, Bolker B, Walker S. Fitting Linear Mixed-Effects Models Using lme4. Journal of Statistical Software. 2015;67(1):1 - 48.
120. Cumming G, Finch S. Inference by eye: confidence intervals and how to read pictures of data. Am Psychol. 2005;60(2):170-80.
121. Cumming G. Inference by eye: reading the overlap of independent confidence intervals. Stat Med. 2009;28(2):205-20.
122. Fox J. Effect Displays in R for Generalised Linear Models. Journal of Statistical Software. 2003;8(15):1 - 27.
123. Fox J, Weisberg S. An R companion to applied regression: Sage publications; 2018.
124. Venables WN, Ripley BD. Modern applied statistics with S. 4th ed: Springer, New York; 2002.
125. Best DJ, Roberts DE. Algorithm AS 89: The Upper Tail Probabilities of Spearman's Rho. Journal of the Royal Statistical Society Series C (Applied Statistics). 1975;24(3):377-9.
126. Team SD. RStan: The R interface to Stan. R package version 2.17. 3. Online: http://mc-stanorg. 2018.